Functional PEG-Modified Thin Films for Biological Detection

Aaron S. Anderson, Andrew M. Dattelbaum, Gabriel A. Montaño, Dominique N. Price,
Jurgen G. Schmidt, Jennifer S. Martinez, W. Kevin Grace, Karen M. Grace, and
Basil I. Swanson*

Los Alamos National Laboratory, Los Alamos, New Mexico 87545

Received October 26, 2007. In Final Form: November 26, 2007

We report a general procedure to prepare functional organic thin films for biological assays on oxide surfaces. Silica surfaces were functionalized by self-assembly of an amine-terminated silane film using both vapor- and solution-phase deposition of 3′-aminopropylmethyldiethoxysilane (APMDES). We found that vapor-phase deposition of APMDES under reduced pressure produced the highest quality monolayer films with uniform surface coverage, as determined by atomic force microscopy (AFM), ellipsometry, and contact angle measurements. The amine-terminated films were chemically modified with a mixture of carboxylic acid-terminated poly(ethylene glycol) (PEG) chains of varying functionality. A fraction of the PEG chains (0.1−10 mol %) terminated in biotin, which produced a surface with an affinity toward streptavidin. When used in pseudo-sandwich assays on waveguide platforms for the detection of *Bacillus anthracis* protective antigen (PA), these functional PEG surfaces significantly reduced nonspecific binding to the waveguide surface while allowing for highly specific binding. Detection of PA was used to validate these films for sensing applications in both buffer and complex media. Ultimately, these results represent a step toward the realization of a robust, reusable, and autonomous biosensor.

Introduction

Surfaces that support the conjugation of a recognition ligand while minimizing nonspecific adsorption of biomolecules are important for biosensing applications.[1,2] Our previous work in this area has focused on using phospholipid bilayer membranes supported on a waveguide-based platform.[3−5] The lipid bilayer architecture has several advantages for biological assays on waveguides, including ease of preparation, low background fluorescence, and excellent specific ligand attachment with suppressed nonspecific binding.[3−5] However, lipid bilayer membranes cannot endure harsh environmental conditions, such as elevated temperature, washing with detergents/denaturing agents, or passage through an air−water interface. Ideally, we would like to prepare functionalized films that maintain the advantages of supported lipid membranes, while minimizing their disadvantages, which primarily involve surface instability. To do this, we focused on modified self-assembled monolayer (SAM) systems of functional alkylsilanes of the type shown in Figure 1, which are based on alkane-thiol SAMs.[6]

It is well-known that alkane-thiol SAMs terminated with poly(ethylene glycol) (PEG) groups can be used to minimize nonspecific binding of biomolecules.[7−11] In contrast, application of PEGylated SAMs on oxide surfaces for biological detection remains an underdeveloped field, despite the potential advantages oxide surfaces afford in terms of useful transduction approaches.[12−15] Further, much of the work involving PEG coatings on oxide surfaces is only concerned with preventing nonspecific
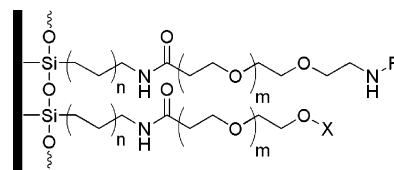

Figure 1. General scheme of a functionalized PEG film; *n*, *m*, *R*, and *X* can all be varied.

biomolecular interactions.[10−12,16−23] Only a few groups have prepared PEG films that simultaneously minimize nonspecific interactions and maximize analyte binding for biosensing applications. For example, Zhen et al.[14,15] have used PEG polymers (>3.4 kDa) functionalized with lysine groups to cover surfaces for targeted sensing applications. However, these films lack covalent attachment to the surface, which makes them unusable when extended storage and reusability are required attributes. Thompson et al.[24] have overcome this issue by using a silane functionalized PEG polymer (MW > 3 kDa) that is covalently

(1) Castner, D. G.; Ratner, B. D. *Surf. Sci.* **2002**, *500*, 28−60.
(2) Lasseter, T. L.; Clare, B. H.; Abbott, N. L.; Hamers, R. J. *J. Am. Chem. Soc.* **2004**, *126*, 10220−10221.
(3) Grace, K. M.; Goeller, R. M.; Grace, W. K.; Kolar, J. D.; Morrison, L. J.; Sweet, M. R.; Wiig, L. G.; Reed, S. M.; Lauer, S. A.; Little, K. M.; Bustos, G. L.; Anderson, A. S.; Swanson, B. I. *Proc. SPIE-Int. Soc. Opt. Eng.* **2004**, *5269*, 55−64.
(4) Martinez, J. S.; Grace, W. K.; Grace, K. M.; Hartman, N.; Swanson, B. I. *J. Mater. Chem.* **2005**, *15*, 4639−4647.
(5) Kelly, D.; Grace, K. M.; Song, X.; Swanson, B. I.; Frayer, D.; Mendes, S. B.; Peyghambarian, N. *Opt. Lett.* **1999**, *24*, 1723−1725.
(6) Love, J. C.; Estroff, L. A.; Kriebel, J. K.; Nuzzo, R. G.; Whitesides, G. M. *Chem. Rev.* **2005**, *105*, 1103−1169.
(7) Palegrosdemange, C.; Simon, E. S.; Prime, K. L.; Whitesides, G. M. *J. Am. Chem. Soc.* **1991**, *113*, 12−20.
(8) Prime, K. L.; Whitesides, G. M. *Science* **1991**, *252*, 1164−1167.
(9) Prime, K. L.; Whitesides, G. M. *J. Am. Chem. Soc.* **1993**, *115*, 10714−10721.
(10) Ma, H. W.; Hyun, J. H.; Stiller, P.; Chilkoti, A. *Adv. Mater.* **2004**, *16*, 338−341.
(11) Ma, H. W.; Wells, M.; Beebe, T. P.; Chilkoti, A. *Adv. Funct. Mater.* **2006**, *16*, 640−648.
(12) Dalsin, J. L.; Lin, L. J.; Tosatti, S.; Voros, J.; Textor, M.; Messersmith, P. B. *Langmuir* **2005**, *21*, 640−646.
(13) Huang, N. P.; Csucs, G.; Emoto, K.; Nagasaki, Y.; Kataoka, K.; Textor, M.; Spencer, N. D. *Langmuir* **2002**, *18*, 252−258.
(14) Zhen, G. L.; Eggli, V.; Voros, J.; Zammaretti, P.; Textor, M.; Glockshuber, R.; Kuennemann, E. *Langmuir* **2004**, *20*, 10464−10473.
(15) Zhen, G. L.; Falconnet, D.; Kuennemann, E.; Voros, J.; Spencer, N. D.; Textor, M.; Zurcher, S. *Adv. Funct. Mater.* **2006**, *16*, 243−251.
(16) Lee, S. W.; Laibinis, P. E. *Biomaterials* **1998**, *19*, 1669−1675.
(17) Meagher, R. J.; Seong, J.; Laibinis, P. E.; Barron, A. E. *Electrophoresis* **2004**, *25*, 405−414.
(18) Papra, A.; Gadegaard, N.; Larsen, N. B. *Langmuir* **2001**, *17*, 1457−1460.
(19) Pasche, S.; Voros, J.; Griesser, H. J.; Spencer, N. D.; Textor, M. *J. Phys. Chem. B* **2005**, *109*, 17545−17552.
(20) Zhang, M. Q.; Desai, T.; Ferrari, M. *Biomaterials* **1998**, *19*, 953−960.
(21) Sharma, S.; Desai, T. A. *J. Nanosci. Nanotechnol.* **2005**, *5*, 235−43.
(22) Sharma, S.; Johnson, R. W.; Desai, T. A. *Langmuir* **2004**, *20*, 348−356.
(23) Sharma, S.; Popat, K. C.; Desai, T. A. *Langmuir* **2002**, *18*, 8728−8731.
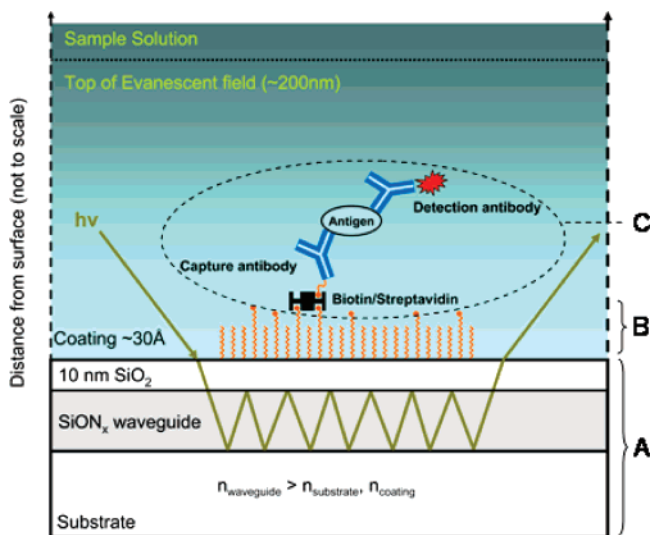
Figure 2. Waveguide architecture (A), surface coating (B), and sandwich assay components (C).

attached to an oxide surface for fluorescence-based biorecognition experiments. Further, Seidel et al.[25] have used patterned amine-functionalized PEG polymers, which are constructed on functionalized short-chain silane monolayers, for multiplexed biosensing applications. Similar work by Majumdar et al. used standard lithography techniques to prepare regions of functionalized silane monolayers for binding of analytes. These functional regions were surrounded by a field of PEG-terminated silanes to prevent both nonspecific binding to the background surface and reagent loss.[26]

To date, no one has characterized or made use of mixed PEG−silane films based on short alkyl chain SAMs and short PEG chains (3−4 PEG units), shown schematically in Figure 2, for biosensing applications on oxide surfaces. There are several advantages to such a surface for sensing applications, including covalent attachment and chemical flexibility. Further, the ratio of PEG-terminated groups that prevent nonspecific interactions (methoxy or hydroxy) and those that can bind analytes, such as biotin or histidine, may be readily modified to maximize specific binding and minimize nonspecific interactions. As such, these films were integrated into sandwich-type assays for detecting *Bacillus anthracis* protective antigen (PA), based on optical transduction methods, which is schematically shown in Figure 2. The films were also useful for assays in complex media (fetal bovine serum (FBS)). Finally, we also found that the covalently attached PEG−silane films described here were stable under a range of environmental conditions. Because these films are regenerable and stable, they are potentially applicable for autonomous sensing platforms.

Experimental Section

Chemicals and Materials. 3-Aminopropyl-1-(methyldiethoxysilane) (APMDES) was purchased from Gelest and used as received. Piperidine, *N,N*-diisopropylethylamine (DIEA), acetone, ethanol (EtOH), phosphate-buffered saline (PBS), and *N*-methylpyrrolidinone (NMP) were purchased from either Sigma-Aldrich or Fisher Chemical and used as received. Toluene was purchased from Acros or Sigma-Aldrich and dried over calcium hydride before use. All discrete, monodisperse polyethyleneglycol (dPEG) reagents were obtained from Quanta Biodesigns, Inc. The entire bottle of each reagent was

diluted to 1 mL with NMP before use. These dilutions gave 1.06 M (250 mg/mL, MW = 236.26 g/mol) HOOC−PEG$_4$−OCH$_3$ and 205 mM (100 mg/mL, MW = 487.54 g/mol) HOOC−PEG$_4$−CH$_2$-CH$_2$−NHFmoc, the use of which are described later in the text. Benzotriazole-1-yl-oxy-tris-pyrrolidino-phosphonium hexafluorophosphate (PyBOP) and *N*-(biotinyloxy)succinimide (Biotin-OSu) were purchased from NovaBiochem. All lipids were used as received from Avanti Polar Lipids, Inc. Streptavidin, FITC−streptavidin, and neutravidin were obtained from Pierce. *B. anthracis* protective antigen and the antibodies against it were purchased from Advanced Immunochemical and were either labeled with a fluorophore (the reporter antibody) or biotin (the capture antibody) for use in sandwich and pseudo-sandwich assays. The UV photomask (chrome on quartz) was designed at Los Alamos National Laboratory and fabricated by Photosciences, Inc. The waveguides were purchased from nGiMAT.

Preparation of Functionalized Silica Films. Silicon wafers with a native oxide (~17 Å) or silicon oxy-nitride (SiON$_x$) waveguides coated with a layer of SiO$_2$ (10 nm) were cleaned by rinsing in ethanol, drying under a stream of argon (Ar), and exposing to deep-UV light (~45 min), which generates ozone and oxygen radicals to remove contaminants from the oxide surface.[27] The clean wafers were rinsed in 18 MΩ/cm water, dried under a stream of Ar, and immediately placed in a glass petri dish along with a small watch glass containing 50 μL of APMDES. The top of the petri dish was placed over the samples to help localize the silane vapor, and then the dish was placed in a vacuum desiccator. The desiccator was evacuated to 125−150 mmHg to evaporate a small amount of the silane and promote vapor deposition on the partially hydrated oxide surface, and was held under static vacuum for ~2−3 h. It was important to maintain a constant distance (~2 in.) between the silane sample and each substrate in the chamber for consistency of the coating process. For solution-phase depositions, freshly cleaned pieces of silicon or glass were immersed in a solution of 0.1−1% silane in dry toluene for 2 h, then rinsed with acetone and ethanol and blown dry with argon. After film deposition by vapor or solution methods, all samples were placed in a 100−120 °C oven for ~30 min. Upon removal from the oven, the films were cooled over drying agent in a desiccator to prevent water condensation, then rinsed with ethanol and dried under a stream of argon.

The amine-coated surfaces were treated with a solution of HOOC−PEG$_4$−NHFmoc (0.1−1 mol %; Fmoc = 9-fluorenylmethoxycarbonyl) and HOOC−PEG$_4$−OCH$_3$ (~99−99.9 mol %) overnight at room temperature. In all cases the coupling reactions employed one of the standard peptide chemistry conditions reported in the NovaBiochem 2006/2007 catalog, namely using DIEA (2 molar equiv relative to the total mols of the PEG reagents) as the base, and PyBOP (0.95 molar equiv) as the carboxylic acid activating reagent in NMP. The Fmoc protecting group was removed with 20% piperidine/NMP (two 15 min treatments) to yield an unprotected amine. Overnight reaction with Biotin-OSu (1 mM) using DIEA (2 mM) as the base in NMP afforded a biotinylated surface for biological assay experiments. For all steps, the films were characterized by Magnetic AC-mode (MAC-mode) atomic force microscopy (AFM, Molecular Imaging Pico Plus II, Type II MAC cantilevers), contact angle measurements (Tantec model CAM-MICRO contact angle meter), and spectroscopic ellipsometry (VASE, J. A. Woollam, Co.).

Patterned Surfaces. Patterned surfaces were prepared by selectively exposing the biotin-functionalized PEG films to deep-UV light through a photomask of chromium deposited on a quartz substrate as described previously.[28] The UV-cleaned regions were back-filled with a vapor-deposited APMDES film, which was coupled to COOH−PEG$_4$−OCH$_3$ using the method described above. These patterned films were exposed to an aqueous solution of fluorescein-labeled streptavidin and characterized by fluorescence microscopy (Olympus IX81 microscope with a FITC filter cube and an Olympus DP71 camera).

(24) Kang, E.; Park, J. W.; McClellan, S. J.; Kim, J. M.; Holland, D. P.; Lee, G. U.; Franses, E. I.; Park, K.; Thompson, D. H. *Langmuir* **2007**, *23*, 6281−6288.
(25) Wolter, A.; Niessner, R.; Seidel, M. *Anal. Chem.* **2007**, *79*, 4529−4537.
(26) Kannan, B.; Castelino, K.; Chen, F. F.; Majumdar, A. *Biosens. Bioelectron.* **2006**, *21*, 1960−1967.

(27) Moon, D. W.; Kurokawa, A.; Ichimura, S.; Lee, H. W.; Jeon, I. C. *J. Vac. Sci. Technol. A* **1999**, *17*, 150−154.
(28) Dattelbaum, A. M.; Amweg, M. L.; Yee, C.; Ecke, L. E.; Shreve, A. P.; Parikh, A. N. *Nano Lett.* **2003**, *3*, 719.
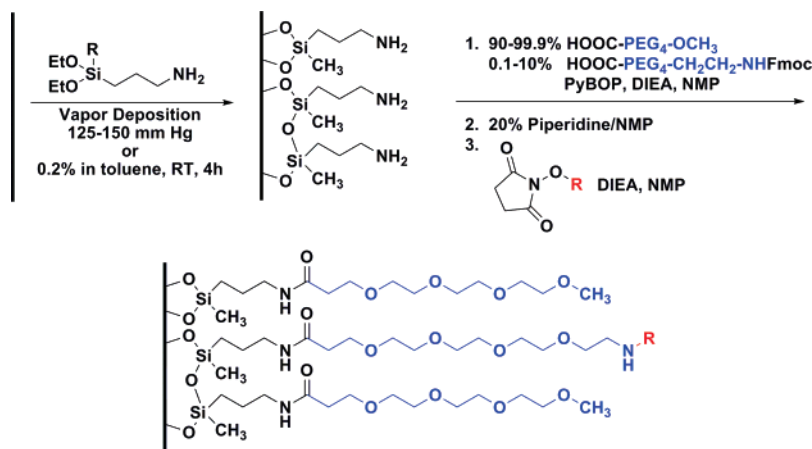
Figure 3. Scheme showing the preparation and modification of functionalized PEG films.

Preparation of Phospholipid Bilayers. Phospholipid bilayers were prepared as previously reported.[4] Briefly, 1,2-dioleoyl-*sn*-glycero-3-phosphocholine (DOPC, 59 μL, 5 mM in CHCl$_3$) and 1,2-dioleoyl-*sn*-glycero-3-phosphoethanolamine-*N*-(cap biotinyl) (sodium salt) (DOGP-CapBiotinyl, 0.6 μL, 5 mM in CHCl$_3$) were combined and the resulting solution was concentrated to a white film under a stream of argon. The lipids were hydrated by suspending the film in 1× PBS (∼0.01 M, pH 7.4) and shaking gently for 30 min. The suspension was subjected to five freeze−thaw cycles (freezing the suspension in liquid nitrogen and allowing it to warm to room temperature) and was disrupted using a probe sonicator; different sonicators require different settings for the same power output, so those settings are not listed here. The vesicle solution was injected into a flow cell assembly (waveguide, gasket, and coverslip with injection ports) and allowed to incubate overnight. The resulting phospholipid bilayer membrane was blocked for 2 h with 2% bovine serum albumin (BSA) in 1× PBS before performing functional assays.

Waveguide Assay. The specific and nonspecific binding to the functionalized PEG surfaces were tested using a previously developed sandwich assay for the detection of protective antigen (PA), which is a marker for *B. anthracis* (anthrax).[4] Different antibodies were chosen for the capture and detection phases of the assays. The capture antibody, 105-anti-PA, was conjugated with biotin in order to facilitate its attachment to streptavidin. The reporter, or detection, antibody, 106-anti-PA, was labeled with Alexa-Fluor 532, a fluorescent dye (Molecular Probes). The numbers 105 and 106 are Advanced Immunochemical catalog numbers and have no further meaning. By choosing different antibodies for the different elements of the assay, we were sure to bind different epitopes of the antigen, thereby eliminating competition for binding sites on the antigen and creating an effective "sandwich."

In some cases, the functionalized waveguides were initially blocked with a 2% BSA/PBS (0.010 M, pH 7.4) solution and rinsed with 0.5% BSA/PBS prior to taking measurements. After assembly into a flow cell, excitation light (532 nm diode-pumped Nd:YAG) was coupled into the waveguide using a diffraction grating that was fabricated into the waveguide architecture. The waveguide background fluorescence spectrum was collected using an Ocean Optics fiber optic spectrometer. Next, solutions of unlabeled neutravidin and biotinylated 105-anti-PA antibody (for antigen capture; ∼0.17 μM, measured by UV−vis spectroscopy) were added to the waveguide surface. Each addition was followed by rinsing with at least 10 aliquots (10× the volume of the flow cell; ∼1.5 mL) of 0.1% Tween-20/PBS. After addition of the capture reagents, another spectrum was collected and compared to the waveguide background to ensure that no changes in fluorescence intensity were observed. To determine the nonspecific binding of the PEGylated waveguide surfaces, 106-anti-PA antibody labeled with Alexa-fluor 532 (∼0.053 μM, measured by UV−vis) was added prior to injection of PA. Finally, PA (1 nM in PBS) and another aliquot of Alexa-fluor 532-labeled-106 were added to determine the level of specific binding to the surface.

Measurements are reported as ratios of the maximum fluorescence intensities observed in a given set of spectra to account for variations in intensity among different waveguides. The measured nonspecific binding (NSB) data are corrected by first subtracting out the fluorescence signal due to the waveguide background spectrum (BG), then dividing by the background signal (BG) to provide a ratio, defined as the corrected nonspecific binding value (NSBc = (NSB − BG)/BG). In a similar fashion, the corrected specific binding (SBc = (SB − NSB)/NSB) takes into account the fluorescence intensity due to nonspecific binding, where SB is the specific binding fluorescence signal measured after PA is added. Here, the uncorrected nonspecific binding signal is subtracted because it includes the signal from the waveguide background. These corrected ratios for nonspecific binding and specific binding allow comparisons of assays on different waveguides, despite systematic variations between experiments.

Results and Discussion

Functional Silane Films. The preparation of our functionalized silane films is schematically summarized in Figure 3. Amine-terminated silane films of APMDES were deposited on silica surfaces by either solution-based deposition or vapor-phase deposition at reduced pressures. Previous accounts have described complete silane monolayer coverages on planar surfaces using solution-phase deposition with rigorously dry solvents[29−32] and/or controlled inert atmospheres.[30,33−36] Although solution-phase depositions of silanes are by far the most widely used techniques for preparing silane SAMs, these methods also generate significant amounts of waste, which is not advantageous economically or environmentally. Vapor-phase deposition of silanes on planar surfaces provides an alternative deposition method that removes the need for solvent use. Several groups have pursued vapor deposition of silanes on planar and porous materials, but they generally rely on high-temperature and/or high-pressure processes.[33,37−44] We found that vapor depositions of short-chain

(29) Howarter, J. A.; Youngblood, J. P. *Langmuir* **2006**, *22*, 11142−11147.

(30) Haller, I. *J. Am. Chem. Soc.* **1978**, *100*, 8050−8055.

(31) Moon, J. H.; Kim, J. H.; Kim, K.; Kang, T. H.; Kim, B.; Kim, C. H.; Hahn, J. H.; Park, J. W. *Langmuir* **1997**, *13*, 4305−4310.

(32) Moon, J. H.; Shin, J. W.; Kim, S. Y.; Park, J. W. *Langmuir* **1996**, *12*, 4621−4624.

(33) Finocchio, E.; Macis, E.; Raiteri, R.; Busca, G. *Langmuir* **2007**, *23*, 2505−2509.

(34) Kurth, D. G.; Bein, T. *Langmuir* **1993**, *9*, 2965−2973.

(35) Kurth, D. G.; Bein, T. *Langmuir* **1995**, *11*, 3061−3067.

(36) Wang, Y.; Ferrari, M. *J. Mater. Sci.* **2000**, *35*, 4923−4930.

(37) Basiuk, V. A.; Chuiko, A. A. *J. Chromatogr.* **1990**, *521*, 29−42.

(38) Ek, S.; Iiskola, E. I.; Niinisto, L. *Langmuir* **2003**, *19*, 3461−3471.

(39) Ek, S.; Iiskola, E. I.; Niinisto, L. *Langmuir* **2003**, *19*, 3461−3471.

(40) Kremer, D. M.; Davis, R. W.; Moore, E. F.; Ehrman, S. H. *J. Cryst. Growth* **2003**, *247*, 333−336.

(41) Lakomaa, E. L. *Appl. Surf. Sci.* **1994**, *75*, 185−96.
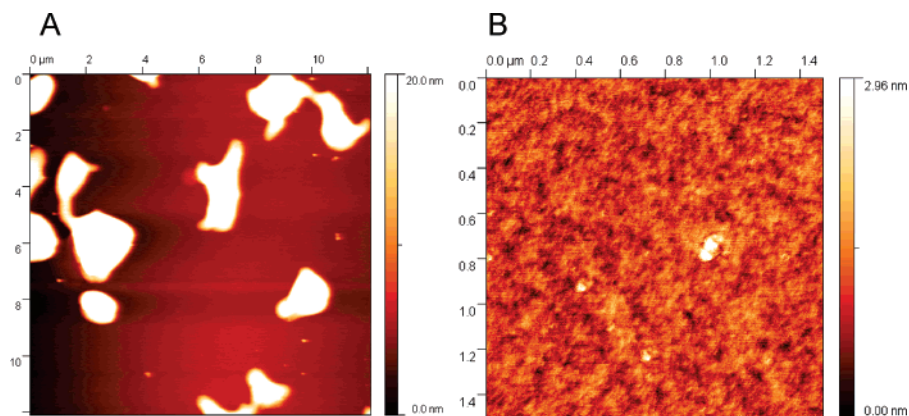
Figure 4. AFM of APMDES silane films deposited (A) from a 1% anhydrous toluene solution or (B) by vapor-phase deposition. Scale bars show scale in the *z* direction (height).

amine-terminated alkylsilanes could be accomplished with relatively mild vacuum (125−150 Torr) and at room temperature to produce thin films of sufficient quality for our detection platform (see assay results below). Water contact angles for these amine coated surfaces ranged from 60 to 65° on either glass or silicon/native oxide with the contact angles on glass being slightly less than those measured on the silicon surfaces. These values were consistent with similar amine-terminated surfaces reported previously.[32] In addition, ellipsometric measurements showed that the film thickness was 10 ± 2 Å for films prepared using APMDES, indicating full monolayer coverage. Solution-phase deposition from toluene yielded similar but inconsistent results, as seen elsewhere.[31,32,45] Thus, when the silane is appreciably volatile, as is the case for APMDES, vapor deposition has become our preferred method for preparing functional silane thin films.

While contact angles and ellipsometric measurements were useful for determining the bulk properties of the deposited films, they did not effectively describe the nanoscale topography of the films, which we found to be a critical factor for successful waveguide-based assays (see below). This analysis required the application of AFM. Significant differences in the film topography were observed depending on the deposition method used (Figure 4). APMDES films deposited from a toluene solution did not completely cover the entire surface, and in many areas formed large aggregated structures and multilayers with sizes ranging from tens of nanometers to micrometers (Figure 4a). In contrast, vapor-deposited films of APMDES were found to completely cover the silica surfaces without multilayer or large aggregate formation. The vapor-deposited APMDES thin films are also less prone to aggregation than vapor-deposited 3′-aminopropyltriethoxysilane (APTES) films as reported previously.[46]

After silane deposition, the resulting amine surface was modified with a mixture of PEG reagents. Previous waveguide assays using lipid bilayers indicated that there was an optimal concentration of biotin for PA assays and that high concentrations of biotin in the lipid bilayers (> 1 mol %) increased nonspecific binding.[4] Therefore, only a small (≤ 1 mol %) percentage of an Fmoc-protected, amine-terminated, PEG-carboxylic acid (for ligand attachment) was co-dissolved with a larger percentage of

a methoxy-terminated PEG-carboxylic acid (for nonspecific binding resistance). Both PEG reagents were attached to the amine by activating the carboxylic acids with PyBOP in NMP. The Fmoc protecting group was removed from the PEG-amine by washing with 20% piperidine in NMP. The deprotection time was kept to a minimum (two treatments of 15 min each) to avoid any side-reactions due to the 9-fluorenyl (dibenzofulvene) radical. The resulting free amine was reacted with the succinimide ester of biotin to create a biotin-functionalized surface (Figure 3). PEG coupling to APMDES SAMs gave a contact angle of ∼50°, indicating conjugation of the PEG species to the surface-bound propylamine. Ellipsometric measurements on dry films only found a 3−5 Å thickness increase, which is much less than we would have expected if the PEG units were well-packed and oriented perpendicular to the surface. Therefore, we presume that the PEG molecules are lying down on the surface, forming a randomly oriented film in a manner similar to a much higher molecular weight PEG polymer. AFM evidence supports this as no large changes can be observed in PEG treated APDMES surfaces (Figure 5a and c). In combination, the decrease in contact angle and the slight increase in film thickness observed ellipsometrically, as well as the lack of large morphological changes in the AFM, indicated that the surfaces were functionalized in a uniform manner (for vapor-deposited APMDES films) and were ready to be tested by functional assays.

Streptavidin Binding Studies. In Figure 5, we show AFM images of various films taken under aqueous conditions before and after exposure to streptavidin, which should have a strong affinity to the biotin-functionalized surface. As seen from the AFM images of the 99% methoxy-PEG/1% biotin-PEG surfaces (Figure 5A and B) and the 100% methoxy-PEG functionalized (Figure 5C and D), binding of streptavidin only occurred on the surface containing a fraction of biotin-terminated PEG. The streptavidin had a measurable height of ∼5 nm, consistent with the crystal structure of this protein.[47,48] Nonspecific binding of streptavidin to the 100% methoxy-PEG functionalized surface or the APDMES surface (data not shown) was not observed. Because the PA sandwich assay involved attachment of capture antibodies to the functionalized surfaces using a biotin−streptavidin linkage, it was important to show that nonspecific absorption of streptavidin will not occur on the biotin-free surfaces. Further, streptavidin binding to the 1% biotinylated surface was well distributed without the appearance of large

(42) Suntola, T. *Mater. Sci. Rep.* **1989**, *4*, 261−312.

(43) White, L. D.; Tripp, C. P. *J. Colloid Interface Sci.* **2000**, *232*, 400−407.

(44) Wikstrom, P.; Mandenius, C. F.; Larsson, P. O. *J. Chromatogr.* **1988**, *455*, 105−117.

(45) Vansant, E. F.; Van Der Voort, P.; Vrancken, K. C. *Characterization and chemical modification of the silica surface*; Elsevier: Amsterdam, 1995; Vol. 93.

(46) Anderson, A. S.; Dattelbaum, A. M.; Montaño, G. A.; Schmidt, J. G.; Martinez, J. S.; Grace, W. K.; Grace, K. M.; Swanson, B. I. *MRS Proc.* **2007**, in press.

(47) Hendrickson, W. A.; Pahler, A.; Smith, J. L.; Satow, Y.; Merritt, E. A.; Phizackerley, R. P. *Proc. Natl. Acad. Sci. U.S.A.* **1989**, *86*, 2190−2194.

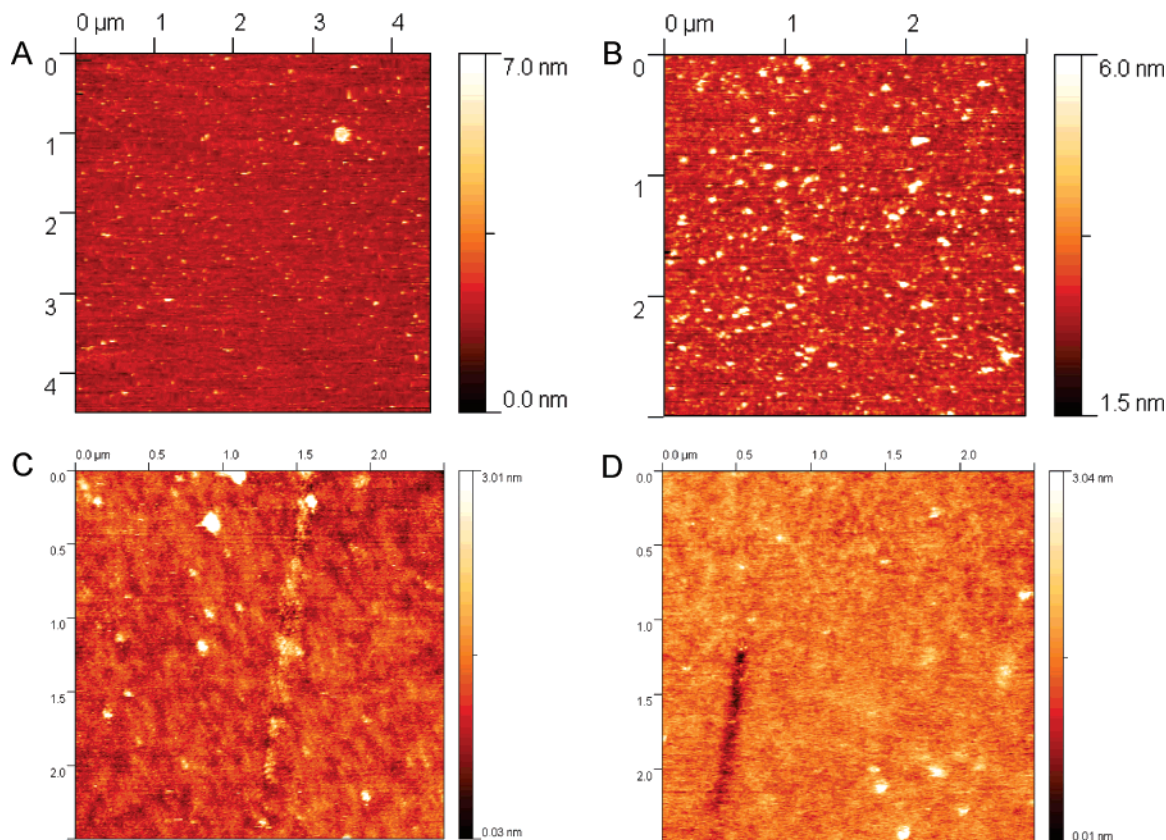(48) Tanaka, S.; Mohri, N.; Kihara, H.; Ohno, M. *J. Biochem.* **1985**, *97*, 1377−1384.

Figure 5. AFM images taken under dd-H$_2$O of a PEG film consisting of 2% PEG-terminated biotin, before (A) and after (B) exposure to a solution of streptavidin. For comparison, AFM images of a PEG functionalized film without biotin are shown before (C) and after (D) exposure to a solution of streptavidin.

aggregation effects (Figure 5B), which indicates that that the Fmoc-protected PEG units are not aggregating together during the coupling reactions to the APMDES SAMs.

We also looked at the functionality and nonspecific absorption properties of a biotinylated-PEG functionalized surface (vapor deposited APMDES) by fluorescence microscopy. A patterned PEG film that contained regions of methoxy-terminated PEG-alkylsilanes and regions containing 1% biotin-terminated PEG silanes was prepared. After treatment with fluorescein-labeled streptavidin, regular patterns were observed with a fluorescence microscope, indicating that the fluorescently labeled streptavidin was only bound to the regions where biotin was present (Figure 6A). Fluorescence images taken on patterned films constructed on amine-terminated SAMs prepared by solution-phase deposition showed similar results. However, when we used the solution-deposited SAMs for waveguide assays, significant amounts of nonspecific binding were observed (see below). Waveguide measurements proved to be more sensitive to nonspecific interactions than fluorescence microscopy experiments.

Waveguide Assays. Waveguides (from nGimat, see Figure 2) consists of a high index of refraction dielectric film (SiON$_x$) sandwiched between two layers of fused silica—a planar substrate and a thin coating. Excitation laser light is coupled into the waveguiding layer through an integrated diffraction grating etched in the surface of the waveguide. Because fused silica has a lower refractive index than SiON$_x$, the light propagates through the high-index material with ~120 reflections per millimeter. The near-total internal reflection in the waveguide provides a strong interaction between the guided light and the surface because a small percentage of the propagated laser light "leaks" out of the waveguide layer creating an evanescent field. The intensity of
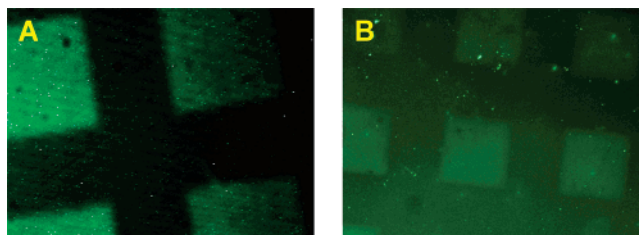

Figure 6. Fluorescence microscopy images of patterned function-alized PEG films constructed on vapor-deposited APMDES after exposure to fluorescently labeled streptavidin. The green squares are regions where the PEG films contain ~1% biotin-terminated PEG, while the darker regions contain no biotin. Image A was captured after incubating the patterned film at room temperature for 2 min in a FITC-streptavidin solution. Image B was captured after incubation of the patterned slide at 80 °C in Leighton-Doi growth media for 60 min, followed by 2 min incubation in a FITC-streptavidin solution.

the evanescent field decays exponentially with distance, with complete loss of intensity at about 200 nm from the waveguide surface.[3-5] Therefore, the bulk solution volume is not irradiated while the field intensity at the surface remains strong. This intensity gradient is important for detecting small amounts of analyte bound to a surface while minimizing background fluorescence from the solution.

The waveguide assay used in this study was similar to an enzyme-linked immunosorbent assay (ELISA), with one major difference: in waveguide assays the capture antibody was specifically bound to the surface rather than nonspecifically adsorbed (Figure 2). This specific binding was carried out by adding an aliquot (2× the volume of the flow cell) of streptavidin
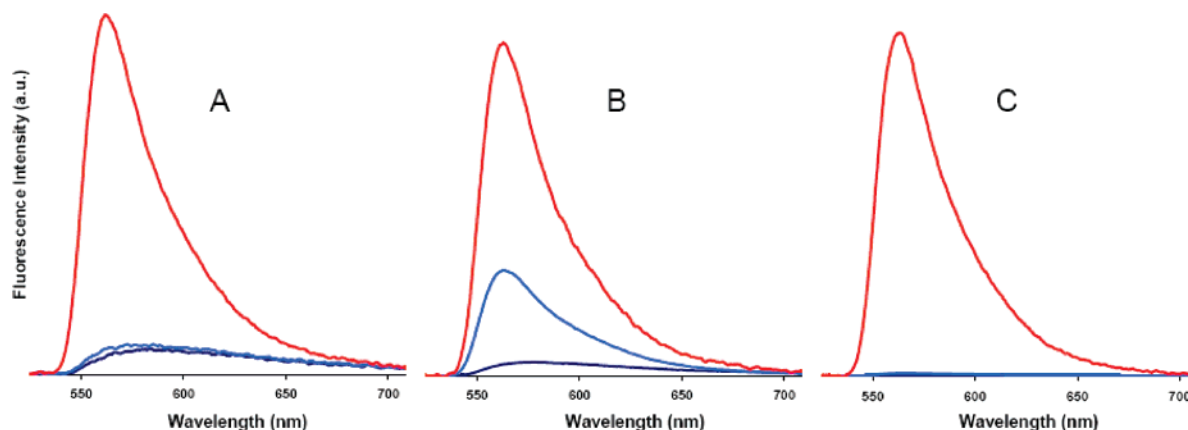
Figure 7. Waveguide-based sandwich assays performed on various functionalized thin films. (A) Supported phospholipid bilayer (99% POPC/1%biotin-DHPE), (B) PEG-functionalized film constructed on a solution-grown APMDES film and (C) PEG-functionalized film constructed on a vapor-grown APMDES film. Color key: background (dark blue), nonspecific binding spectrum (light blue), and specific binding spectrum (red).

Table 1. Typical Binding Data for PA Assays

entry	surface/experiment[a]	nonspecific binding (NSBc)[b]	specific binding (SBc)[b]
1	phospholipid bilayer/PA binding (Figure 7A)	0.27	52
2	solution-grown APMDES/PA binding (Figure 7B)	6.8	2.4
3	V.D.[c] APTES, blocked[d] 1 h/PA binding[e]	29	79
4	V.D. APTES, blocked[d] overnight/PA binding[e]	0.8	102
5	V.D. APMDES/PA binding (Figure 7C)	1.3	203
6	V.D. APMDES/1 pM PA binding	1.2	0.82
7	V.D. APMDES/10 pM PA binding	1.2	4.9
8	V.D. APMDES/100 pM PA binding	1.2	48
9	V.D. APMDES/PA in bovine serum	3.1	39

[a] All experiments detect 1 nM PA unless otherwise noted. [b] See Experimental Section for NSBc and SBc calculations. [c] V.D. = vapor deposited. [d] Blocked = incubated with 2% bovine serum albumin (BSA). [e] See ref 21.

or neutravidin to the biotinylated surface followed by an aliquot of biotinylated capture antibody. These steps formed the capture surface, and a background fluorescence spectrum was acquired at this point. It was also important to determine the propensity of proteins to stick to this surface in the absence of PA (nonspecific binding). To measure how much nonspecific binding occurred on these surfaces, an aliquot of the fluorescently labeled reporter antibody was added to the flow cell, followed by a rinsing step prior to taking a fluorescence measurement. If the antibody stuck to the surface nonspecifically, the fluorophore was close enough to the surface to be excited by the evanescent field. The amount of fluorescence given by such an experiment gave a quantitative determination of the amount of nonspecific binding. The specific binding efficiency was then determined by adding protective antigen and another aliquot of the reporter antibody. Each addition was followed by washing with 0.1% Tween-20/1× PBS and 1× PBS.

The fluorescence spectra resulting from PA assays (1 nM PA) conducted on various functional waveguide surfaces are shown in Figure 7. In addition, a list of typical corrected specific and nonspecific binding values for each assay reported here is shown in Table 1. For simplicity, these values were calculated using the maximum fluorescence signal found for each measured spectrum. In Figure 7A (Table 1, Entry 1), results from a typical PA detection assay performed on a waveguide coated with a 1% biotin-PE/99% DOPC bilayer are shown. Figure 7B and C (Table 1, Entries 2 and 5) shows PA detection assays performed on waveguides functionalized with PEG films assembled on solution or vapor grown APMDES SAMs, respectively. Functionalized PEG films built on solution-grown, silane-based SAMs were

clearly inferior with respect to nonspecific and specific binding when compared to the lipid bilayers. The NSBc for PEG films assembled on solution grown APMDES SAMs was ~6.8, compared to 0.3 for lipid bilayers, while the SBc ratio on this PEG surface was ~2.4, compared to 52 for a similar PA detection assay done using the lipid bilayer. Adding an auxiliary protein (BSA) in an attempt to block nonspecific binding on this PEG surface had very little effect on the ratios (data not shown). The high nonspecific binding to this functionalized PEG film can be explained by the poor quality of the initial solution-grown APMDES film as seen by AFM (Figure 4A). Significant regions of the waveguide surface remained unfunctionalized, which allowed antibodies to directly adsorb to bare silica.

Waveguide-based PA detection assays performed on PEG-films in which the APMDES film was prepared by a vapor-phase deposition were much more effective at preventing nonspecific binding than PEG-films assembled on APMDES films prepared by a solution-phase deposition method, as seen in Figure 7C. The NSBc ratio (~1.3) was only slightly higher than that measured for BSA blocked lipid bilayers, while the SBc (~203) was much greater. The low nonspecific binding numbers found for these films can be correlated to the uniform surface coverage obtained with the APMDES vapor deposition process (see Figure 4B). Further, in previous work[46] we performed waveguide-based assays on PEG-functionalized films beginning with a vapor deposited APTES films. However, to get results similar to those shown for the APDEMS films in Figure 7C, we needed to block with BSA for several hours prior to the assay. Again, the performance of the PA detection assay can be correlated to the quality of the initial APTES vapor deposited film, which
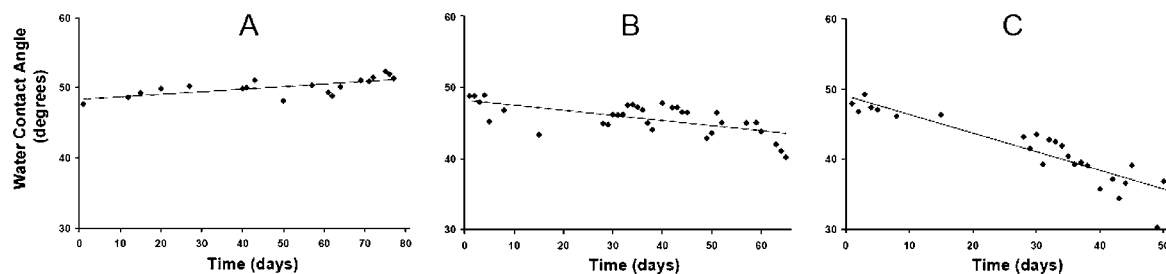
Figure 8. Water contact angles measured on a 1 mol % biotin-functionalized PEG film constructed on a vapor deposited APMDES film deposited on Si plotted as a function of time when stored in (A) air; (B) water, or (C) 1× PBS. Trendlines are included to more clearly illustrate contact angle changes with storage time.

had significant multilayer formation and lacked uniformity as observed by AFM.[46] Thus, assays on functionalized PEG films built on vapor-deposited APMDES are also advantageous because they avoid a blocking step with BSA, which can add up to 12 h of time to the assay. In addition, because there are no large BSA proteins bound to these surfaces, there may be more biotin sites available for binding to streptavidin. An increased concentration of streptavidin on the surface could explain why the SBc signals are higher for the functionalized PEG films compared to assays done on lipid bilayer films.

With initial binding results in hand, we tested the detection limits of the functionalized PEGylated surfaces built on vapor-deposited APMDES films. We found that the limit of detection for PA on these surfaces was between 1 and 10 pM, as shown in Table 1, Entries 6 and 7. At 1 pM PA concentration, the SBc was only ~0.8, indicating an insignificant difference between specific and nonspecific binding. For 10 pM PA, however, the SBc was ~4.9, which is well above the nonspecific binding signal. The SBc value increased significantly with each additional concentration increase (~48 for 100 pM PA, Table 1, Entry 8). These data are similar to the limits of detection for waveguide-based assays using BSA-blocked lipid bilayers.

Assays in Complex Media. PA detection assays were also performed in complex media using PEG-functionalized films constructed on vapor-deposited APMDES SAMs. Our goal was to ensure the stability and binding resistance of these thin films to any interfering proteins that may be present in a biologically relevant sample. To this end, FBS was spiked with PA (1 nM) and was used in binding assays. This media caused a slight increase in the nonspecific binding signal (NSBc = 3.1) while the specific binding signal remained strong (SBc = 39, Table 1, Entry 9). These data are very similar to the signals observed with BSA-blocked lipid bilayers in buffered water. The serum itself contained no fluorescent entities that could not be removed by rinsing with Tween-20 (data not shown). However, the increase in nonspecific binding may indicate that some of the proteins in the serum had an affinity for the PEG surface and may have caused subsequent nonspecific binding of the reporter antibody.

PEG-Functionalized SAM Stability. As we assessed the functionality and quality of the functionalized PEG films, we also evaluated their stability. Ideally, sensor elements coated with the films reported here could be stored for weeks to months and used in complex fluids and under harsh conditions. Thus, two stability experiments were performed. In the first stability experiment, patterned and nonpatterned PEG films constructed on vapor-deposited APMDES were assembled on glass slides and immersed in bacterial growth media (Leighton-Doi) at elevated temperatures—50, 80, and ~95 °C (the boiling point of water at Los Alamos, NM)—for 5, 30, and 60 min. Contact angles were measured on the nonpatterned surfaces and microscopy images were captured after treating the patterned slides with

FITC-streptavidin. The fluorescence pattern observed after 60 min incubation at 80 °C in growth media is shown in Figure 6B. The pattern quality did not change relative to films incubated at lower temperatures, and the film's stability was confirmed by only a slight decrease in the measured contact angle. In boiling media, however, degradation of the surface was observed, both in the quality of the pattern seen by fluorescence microscopy and by a ~5° decrease in the contact angle (data not shown) similar to other PEG-silane films.[22] Taken together, these data demonstrate adequate film stability at elevated temperature in complex media, but with marked instability in boiling media.

In the second stability assessment, PEG-functionalized films attached to vapor deposited APMDES were prepared on glass slides and stored in the dark in air, water, or 1× PBS. The slides were stored in the dark to remove the possibility of light-induced degradation of the PEG chains. Contact angle measurements shown in Figure 8 were taken in an attempt to observe any degradation that occurred. The samples stored in air showed no degradation after seventy-five days; in fact, the contact angle increased slightly (~1% change), indicating possible surface contamination from dust, oils, or microbes in the air. However, the samples stored in water and PBS both showed signs of degradation over time as observed by a ~3% or ~30% decrease in the measured contact angle for water or buffer, respectively. Most likely, the reduced contact angle resulted from hydrolysis of the silane film. Previous results showed that a drop in contact angle was accompanied by a corresponding increase in nonspecific binding during waveguide-based assays of PA (data not shown), confirming our conclusion that contact angle is a straightforward measurement to assess the potential performance of a film for waveguide assays.

Summary

We have demonstrated a facile route to thin films that minimize nonspecific binding while allowing specific attachment of capture elements for biosensor applications. The functionalized PEG coatings effectively minimize nonspecific binding in waveguide-based sandwich assays for the detection of PA both in buffer solutions and in complex media. Furthermore, we demonstrated that the films are relatively stable under a variety of solvents and temperatures, which allows us to consider regeneration of these surfaces for tandem assays on the same waveguide. Efforts toward regeneration are currently underway. The surface functionalization procedures described here use readily available starting materials and known chemistry—amide-bond forming reactions on vapor deposited amine-terminated silane films. In addition, the films may be readily optimized for a variety of different sensing assays. We are currently working on applying these films to other targets, including antigens that indicate different disease/biothreat agents, nucleic acids, and intact organisms. Ultimately, the results

presented here represent a step toward the realization of robust, reusable, and autonomous biosensors.

LA7033438